Quartz tuning fork vibration amplitude as a limitation of spatial resolution of shear force microscopes

J.-M Friedt, É. Carry, Z. Sadani, B. Serio, M. Wilm, S. Ballandras
FEMTO-ST, 32 avenue de l'Observatoire, 25040 Besançon Cedex, FRANCE

Abstract

We compare experimental and finite element modeling of the vibration amplitude of tip-loaded quartz tuning forks. We demonstrate under which experimental conditions the vibration amplitude might become a limiting factor of the lateral resolution of a shear force microscope. Namely, with large excitation amplitudes (> 1 V_{pp}) and under the condition of working at maximum amplitude (as opposed to minimum phase) the displacement amplitude of the tip can be greater than 100 nm, beyond the usual spatial resolution aimed at by scanning probe microscopes (SPM).

1 Introduction

Since Karrai *et al.* [1, 2] showed that quartz tuning forks can be used as sensitive force sensors [3, 4] for scanning probe microscopies [5], many experiments have been developed which monitor various properties of the resonator as a function of the interaction between a tip glued to one prong of the fork and a surface. The spatial resolution of those microscopes are usually attributed to the size of the tip. We wish here to check under which conditions the vibration amplitude of the prongs of the tuning fork might become a limitation of the spatial resolution of scanning probe microscopes.

2 Finite Element Analysis modelling

While a bare, symmetrical quartz tuning fork is accurately modelled as coupled oscillators, finite element analysis [6, 7] is necessary when an additional disturbance such as a tip is asymmetrically attached to one of the prongs. We have first validated our simple quartz tuning fork model with experimental data based on dimensions measured under scanning electronic microscope and tabulated material constants [8, 9]. We have then extended this model by adding tips along one prong with various mechanical properties as used in experiments: either the tip is made of glass (optical fiber) assumed to have mechanical properties similar to that of quartz, of the tip is made of platinum.

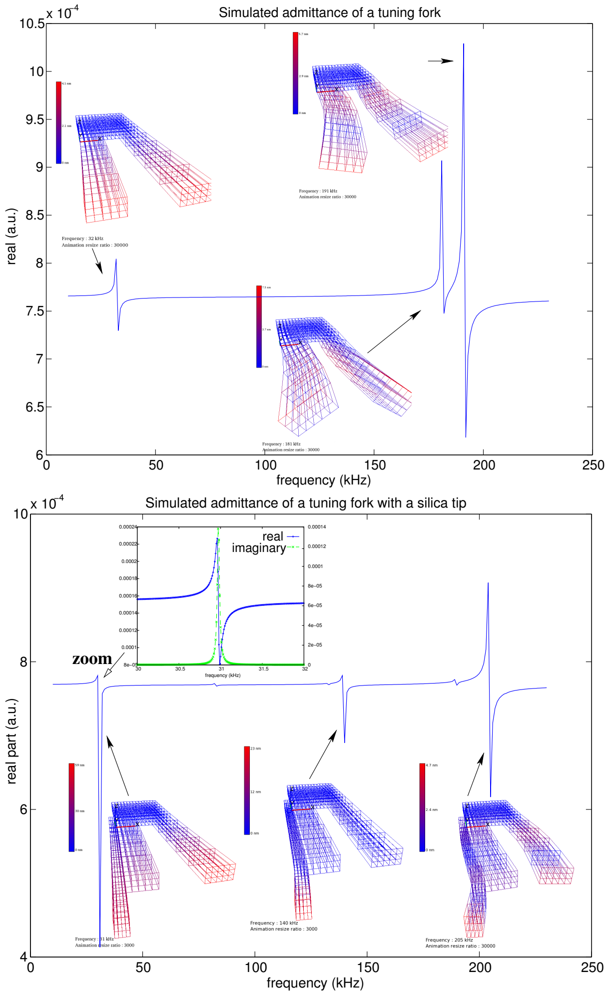

Figure 1: Top: impedance magnitude plot of the bare quartz tuning fork in the 10 to 230 kHz range. The quality factor was taken to be 1000, the driving voltage 0.5 V. The fundamental flexion mode around 33 kHz, the first torsional mode at 181 kHz and the flexion harmonic around 191 kHz are clearly visible. Insets: displacement of the tuning fork. Bottom: same plots for a silica fiber-loaded tuning fork. The asymmetry of the fundamental mode is due to the poor frequency resolution due to limited computation time. Notice the additional mode around 140 kHz which is a resonance of the protruding tip and strongly dependant of the bonding conditions between the fiber and the tuning fork. The 181 kHz torsional mode visible on the bare tuning fork plot has probably been strongly attenuated by the asymmetry due to the glued fiber.

The model is validated by computing the resonance frequencies of the system. An extended version of Modulef (INRIA, France) developed at our institute [10] has been used for computing the electrical impedance and mechanical motion of the piezoelectric device under consideration for a range on frequencies (Fig. 1). We observe (Fig. 1) as expected the resonances around 32 and 191 kHz [11]. These resonances are associated with maximum displacement amplitudes at the end of the prongs of 110 and 20 nm respectively ($Q = 1000$, 0.5 V driving voltage). An analysis over such a wide range of frequency is incompatible in terms of computation time with the high frequency resolution required by the high quality factor experimentally observed ($Q \simeq 1000$) and included in the model as the division factor between real and imaginary parts of the material constants. Hence zooms were performed around the fundamental resonance frequency in order to provide an accurate result independent of the frequency step of the analysis; as seen in inset of Fig. 1.

The linear dependence of the displacement amplitude with the quality factor of the resonator and the driving amplitude have been verified by modelling the tuning fork with quality factors of 1000 and 10000 (leading to a 10 fold increase of the vibration amplitude) and a driving voltage of 0.1 and 0.5 V.

We observe that a quartz tuning fork with one prong loaded with an optical fiber along its length will display a vibration amplitude of the tip of 55 nm when excited at 0.5 V, assuming a quality factor $Q = 1000$ as experimentally observed. This maximum displacement amplitude is reduced to 17 nm if the optical fiber is replaced by a platinum wire of similar dimensions.

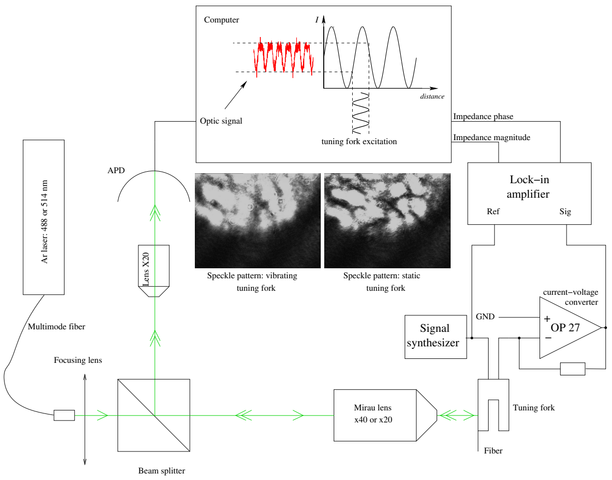

Figure 2: Experimental setup for measuring the displacement of one prong of the quartz tuning fork. Inset: speckle pattern as seen by the photodetector (APD) with a static and a vibrating tuning fork. The blur is due to the integration time of the CCD camera as the tuning fork was vibrating around 32 kHz.

3 Experimental results

3.1 Interferometric method

We have developed a speckle interferometer [12, 13, 14] (Fig. 2) for validating the amplitude informations extracted from finite element modeling. The main issue with the experimental measurement of the vibration amplitude of the quartz tuning fork are :

- the surface roughness of the electrodes which has been measured to be in the 3 to 10 μm range peak to peak. This very large roughness associated with the long coherence length of the Ar laser used implied the use of speckle interferometry
- the large observed amplitudes (under extreme working conditions) – above $\lambda/2$ where $\lambda \simeq 488$ or 514 nm – require an unusual processing step due to folding of the sine-shaped signal over the non-linear interference pattern.

We have varied two parameters: the excitation amplitude (the greater the electrical excitation amplitude, the better the signal to noise ration but the larger the displacement of the tip: Fig. 3) and the excitation frequency in order to be able to link the electrical properties of the tuning fork to mechanical displacements and hence predict the tip displacement without the need for the in-situ interferometric monitoring during actual SPM experiments (Fig. 4). In the latter case, one concludes that whatever the SPM tip-sample feedback mode (working at constant output current magnitude or phase) within the resonance range, the vibration amplitude of the prongs is important over the whole width of the resonance: although our conclusions focus on the maximum vibration amplitude, it can be extended to any feedback method of the tip-sample distance (including feedback of the tip-sample distance for keeping the electrical phase constant).

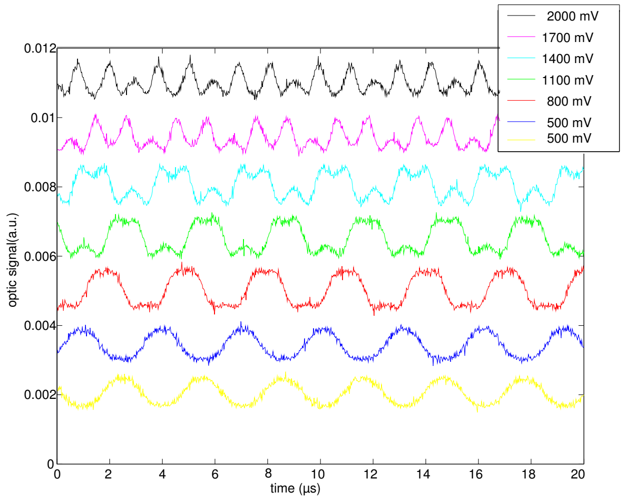

Figure 3: Experimental results of the vibration amplitude as a function of excitation voltage at maximum magnitude frequency

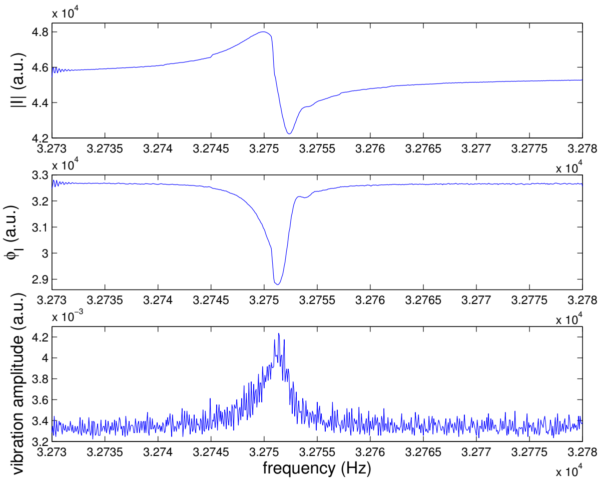

Figure 4: Experimental results of the vibration amplitude as a function of excitation frequency over a range of 50 Hz.

4 Data processing: linking model and experimental data

Data processing of the raw experimental data is performed in the following way :

- for each excitation amplitude a periodically sampled data set has been acquired (sampling rate: 5 Msamples/s, 16 bits/sample)
- each data set is Fourier transformed
- the power of the fundamental frequency components ($f_0 \simeq 32750$ Hz) and of the overtones (due to the non-linear intensity-distance relationship) are computed
- in parallel to processing the experimental data, we simulate the folding of the sine-shaped optical path difference $\delta \propto \omega t$ (with ω the pulsation of the acoustic signal and t the time) over the interference pattern: we obtain an intensity as seen by the photodetector shaped as $\sin(\frac{2\pi}{\lambda} A \sin(\omega t) + \varphi)$, with A the vibration amplitude of the tuning fork and φ a constant offset of the average position of the tuning fork with respect to the linear region of the interference pattern. Here again for each value of A we compute the Fourier transform and extract the Fourier components of the first overtones. We observe that the fundamental and third components are characteristic of the amplitude A while the second component is mostly determined by φ. The only free parameters of this model are the range of A and the phase offset φ.
- from a comparison of the ratio of the powers at the fundamental frequency and overtones (n$\times f_0$, n=[2, 3]) as seen from experimental and simulated data, we extract the quantitative vibration peak-to-peak amplitude in terms of probing laser wavelength: the range of A that best fits our experimental data provides an estimate of the vibration amplitude of the prong under investigation.
- the quantitative peak-to-peak amplitude is obtained from the conversion of the incoming laser wavelength to nanometers (Ar lasers generate two strong signals at either 488 or 514 nm – both have been used in various experiments)

Figs. 5 and 6 display the result of data processing of the experimental data for a bare tuning fork and an optical fiber loaded prong respectively, and a comparison with the modeled power spectrum of a sine wave of varying amplitude folded over the interference pattern. These experimental data display a motion of the cantilever inferior to the one expected from finite element modelling: the latter leads us to predict a peak to peak amplitude for a bare resonator of 174 nm displacement at 0.4 V for a Q=1000 resonator while we experimentally observe a displacement of about 46 nm. Such a result would be consistent with an exceptionally low Q=265 resonator in air which could be attributed to the aging of the electrodes exposed for several weeks to air. The optical fiber loaded tuning fork experimentally displays a vibration amplitude of 11 nm for an excitation voltage of 0.5 V while finite element analysis of a $Q = 1000$ resonator lead us to expect an amplitude of 110 nm for the same driving voltage amplitude. The experimental result would be consistent with a $Q \simeq 100$ while we experimentally observe $Q = 6700$ for this particular setup.

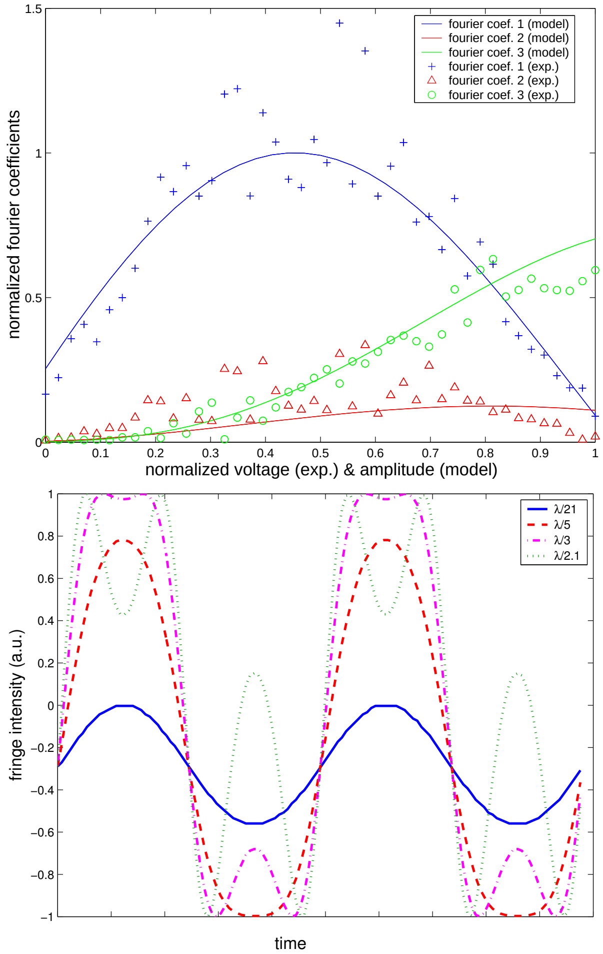

Figure 5: Top: fit of the experimental data to a model of sine wave folding over the interference pattern for extracting quantitative displacement data. The abscissa is graduated in voltage from 400 to 9000 mV (experimental data), which is also equal to (simulated data) a vibration amplitude of $\lambda/21 = 23$ nm to $\lambda/1.7 = 290$ nm ($\lambda = 488$ nm in this experiment). Bottom: result of the model of the folding of the incoming sine wave optical signal over the interference pattern as shown in Fig. 2. Compare with the experimental curves displayed Fig. 3

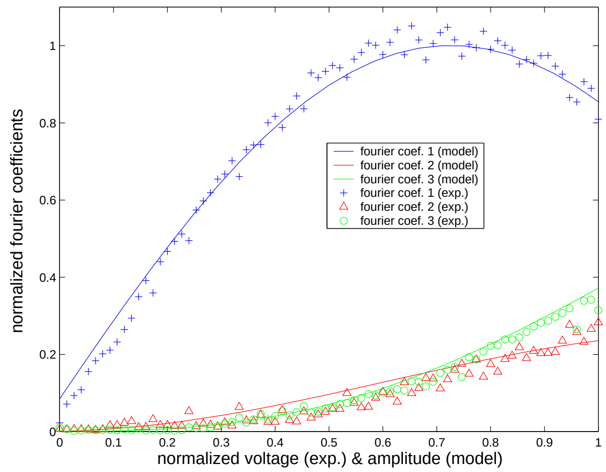

Figure 6: Comparison of the experimental data obtained using an interferometric method on a metallized fiber (the surface of the fiber is smooth enough to obtain here interference fringes rather than speckles) and a model as described in the text. The abscissa spans from 100 mV to 7600 mV amplitude (experiment) which is also equal to $\lambda/126$=4 nm to $\lambda/5$=97 nm (here $\lambda = 488$ nm).

4.1 Stroboscopic method

An alternative to interferometry is to use stroboscopic digital image sampling for measuring the displacement of a surface parallel to the place of the camera sensor [15]. In order to detect minute displacement as required by our application, sub-pixel resolution is obtained by applying an intercorrelation between images of different phase with respect to the oscillation of the tuning fork after interpolation of the images [16].

In this experiment the quartz tuning fork is probed by a square wave signal. Four images phase-synchronized with the oscillation of the tuning fork are taken for each period (Fig. 7).

The result of such a measurement, although sensitive to the roughness of the surface and the induced blurred area of the image due to limited field depth of the microcoscope lens, are as follow : for a peak to peak applied voltage of 0.5 V_{pp} (1.8 V_{pp}, 5 V_{pp} respectively), the displacement amplitude is observed to be 350 nm (850 nm, 3000 nm) as shown Fig. 8. These measurements were performed on a different tuning fork than the one used in the previous experiments, as would be compatible with a resonator with quality factor $Q = 4500$.

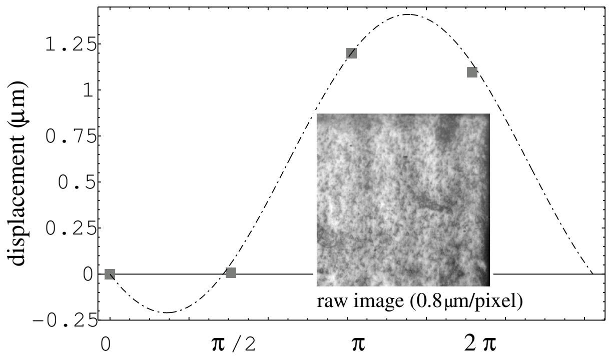

Figure 7: Example of a fit of the sine wave motion of the end of a cantilever powered by a 1.8 V_{pp} square wave. The four squares are the experimental data and the sine wave the fit from which a vibration amplitude of 750 nm is deduced at this pixel position. Inset: one of the four raw images acquired of the surface of the end of a prong: note the obvious roughness of the surface which seems to degrade the resolution of the method.

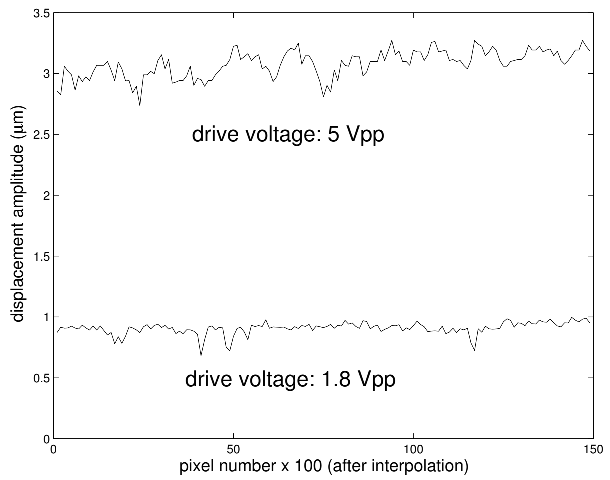

Figure 8: Peak to peak motion of the end of the prong of a tuning fork powered by 1.8 V_{pp} and 5.0 V_{pp} square voltages as computed for all pixels of the image following the method shown Fig. 7. These curves display a standard deviation of 50 nm and 110 nm respectively.

5 Conclusion

We have shown that under many circumstances the vibration amplitude of the quartz tuning fork prong to which the sensing tip of a shear-force microscope is attached might limit the spatial resolution of the scanning probe microscope to a few tens of nanometers, well above the spatial resolution obtained with conventional (contact or tapping) mode atomic force microscopes. These results have been obtained from measurements on bare quartz tuning forks and from preliminary results obtained from tuning forks with one prong loaded with an optical fiber. Experimental results on the bare tuning fork are in agreement with finite element modeling, so that we can confidently extend our finite element analysis of silicate and Pt fiber loaded tuning fork to the same conclusion.

Experimental confirmation of the data computed using finite element analysis software is still needed. A promising extension of this work is the quantitative analysis of the tip-sample interaction by means of electrical impedance recording as well as optical interferometric monitoring of the vibration amplitude. Such interactions can then be compared to classical models of external forces acting on the tip included in the finite element analysis software package.

Acknowledgments

We acknowledge the work of J.-J. Hunsinger (FEMTO-ST, Montbéliard, France) for the development of the electronics of the stroboscopic measurement method.

References

[1] K. Karrai and R.D. Grober, *Piezoelectric tip-sample distance control for near field optical microscopes*, Appl. Phys. Lett. vol 66, num 14, pp.1842-1844, April 1995

[2] Y.-H. Chuang, C.-J. Wang, J.-Y. Huang and C.-L. Pan, *Nonoptical tip-sample distance control for scanning near-field optical microscopy*, Appl. Phys. Lett. vol 69, num 22, pp.3312-3314, November 1996

[3] F.J. Giessibl, *Atomic resolution on Si(111)-(7×7) by noncontact atomic force microscopy with a force sensor based on a quartz tuning fork*, Appl. Phys. Lett. vol 76, num 11, pp.1470-1472, March 2000

[4] Y. Seo, W. Jhe and C.S. Hwang, *Electrostatic force microscopy using a quartz tuning fork*, Appl. Phys. Lett. vol 80, num 23, pp.4324-4326, June 2002

[5] D. Courjon and C. Bainier, *Le champ proche optique : théorie et applications*, Springer (2001) [in French]

[6] R. Arinero and G. Lévêque, *Vibration of the cantilever in Force Modulation Microscopy analysis by a finite element model*, Rev. Sci. Instrum. vol 74, num 1, pp.104-111, January 2003

[7] H. Hantz, F. Sthal and R. Bourquin, *Model for a quartz-crystal tuning fork with coupling between the arms*, in Proceedings of 18^{th} EFTF, 2004

[8] R. Bechmann, A.D. Ballato and T.J. Lukaszek, *Higher order temperature coefficients of the elastic stiffness and compliances of alpha-quartz*, in Proceedings of IRE, pp. 1812-1822, August 1962

[9] Dubois99 (EPFL)

[10] P.F. Edoa, S. Ballandras and M. Wilm, *A finite-element/boundary-element method for the modeling of piezotransducer radiation in fluids using a polynomial development of the Green's function*, J. Acoust. Am. vol 115, num 6, pp.2974-2953, June 2004

[11] V.A. Bykov, S.A. Saunin, I.V. Duskin and A.V. Mezin, *Second mode (190 kHz) of the vibration of the tuning fork application in shear-force measurements*, in Proceedings of the SPM-2002, 2002, pp.258-260

[12] T.R. Moore, *A simple design for an electronic speckle interferometer*, Am. J. Phys. vol 72, num 11, pp.1380-1384, 2004

[13] C. Shönenberger and S.F. Alvarado, *A differential interferometer for force microscopy*, Rev. Sci. Instrum. vol 70, num 10, October 1989

[14] P.G. Gucciardi, G. Bachelier, A. Mlayah and M. Allegrini, *Interferometric measurement of the tip oscillation amplitude in apertureless near-field optical microscopy*, Rev. Sci. Instrum. vol 76, web reference 036105 (2005)

[15] B. Serio, J.-J. Hunsinger and B. Cretin, *In-plane measurements of microelectromechanical systems vibrations with nanometer resolution using the correlation of synchronous images* , Rev. Sci. Instrum. vol 75, num 10, pp.3335-3341, October 2004

[16] H. Foroosh, J.B. Zerubia and M. Berthod, *Extension of phase correlation to subpixel registration*, IEEE transactions on image processing, vol 11, num 3, pp. 188-200, March 2002